

# Journal of Biomedical Optics

[SPIEDigitalLibrary.org/jbo](http://SPIEDigitalLibrary.org/jbo)

## **Detection of rheumatoid arthritis by evaluation of normalized variances of fluorescence time correlation functions**

Thomas Dziekan  
Carmen Weissbach  
Jan Voigt  
Bernd Ebert  
Rainer Macdonald  
Malte L. Bahner  
Marianne Mahler  
Michael Schirner  
Michael Berliner  
Birgitt Berliner  
Jens Osel  
Ilka Osel

# Detection of rheumatoid arthritis by evaluation of normalized variances of fluorescence time correlation functions

Thomas Dziekan,<sup>a</sup> Carmen Weissbach,<sup>a</sup> Jan Voigt,<sup>a</sup> Bernd Ebert,<sup>a</sup> Rainer Macdonald,<sup>a</sup> Malte L. Bahner,<sup>b</sup> Marianne Mahler,<sup>b</sup> Michael Schirner,<sup>b</sup> Michael Berliner,<sup>c</sup> Birgitt Berliner,<sup>d</sup> Jens Osel,<sup>e</sup> and Ilka Osel<sup>e</sup>

<sup>a</sup>Physikalisch-Technische Bundesanstalt, Abbestr. 2-12, 10587 Berlin, Germany

<sup>b</sup>Mivenion GmbH, Robert-Koch-Platz 4, 10115 Berlin, Germany

<sup>c</sup>HELIOS Klinikum Berlin-Buch, Department of Physical Medicine and Rehabilitation, Schwanebecker Chaussee 50, 13125 Berlin, Germany

<sup>d</sup>HELIOS Research Center, Friedrichstraße 136, 10117 Berlin, Germany

<sup>e</sup>Helios Klinikum Bad Saarow, Traumatologie und Orthopädie, Pieskowerstraße 33, 15526 Bad Saarow, Germany

**Abstract.** Fluorescence imaging using the dye indocyanine green as a contrast agent was investigated in a prospective clinical study for the detection of rheumatoid arthritis. Normalized variances of correlated time series of fluorescence intensities describing the bolus kinetics of the contrast agent in certain regions of interest were analyzed to differentiate healthy from inflamed finger joints. These values are determined using a robust, parameter-free algorithm. We found that the normalized variance of correlation functions improves the differentiation between healthy joints of volunteers and joints with rheumatoid arthritis of patients by about 10% compared to, e.g., ratios of areas under the curves of raw data. © 2011 Society of Photo-Optical Instrumentation Engineers (SPIE). [DOI: 10.1117/1.3599958]

Keywords: rheumatoid arthritis; fluorescence imaging; two hand imager; clinical study; correlation function; image interpretation; computer aided diagnostics.

Paper 11108R received Mar. 8, 2011; revised manuscript received May 11, 2011; accepted for publication May 23, 2011; published online Jul. 6, 2011.

## 1 Introduction

Rheumatoid arthritis (RA) is a long lasting disease which irreversibly degrades joints. The medical treatment currently available can only delay or stop the progression of the disease.<sup>1,2</sup> Therefore, early identification of inflammatory destructive processes is important to prevent joint destruction with the help of corresponding therapies.<sup>3</sup> However, the most common imaging method, radiography, is not sensitive enough to detect small changes in early stages of the disease. Although it has been shown that a dynamic MRI could serve as a quasi-gold standard in this respect, in principle, it is rather expensive and not available all over.<sup>4</sup> Recent work<sup>5-7</sup> about the utilization of contrast-enhanced near-infrared (NIR) imaging techniques for detection of rheumatoid arthritis has therefore attracted noticeable interest.

A pilot clinical trial showed that an NIR imaging system, in combination with the dye indocyanine green (ICG), has the potential for routine clinical application.<sup>8</sup> ICG can be used to spot the higher vascularization in inflamed tissue of joints affected by rheumatoid arthritis.<sup>9</sup> Due to its protein binding properties to albumin, it does not show extravasation for concentrations < 0.5 mg/ml (serum).<sup>10-13</sup> Encouraged by the promising results of the above-mentioned pilot clinical trial, a prospective clinical study with an increased number of participants was conducted. The imaging system applied for this purpose allows a detailed real-time recording of the in- and outflow of an injected ICG bolus in both hands detecting the fluorescence radiation emitted

by the circulating dye molecules after optical excitation. The challenge here is to distinguish between normal variations of the vascular system in healthy volunteers and abnormalities due to inflammatory processes of RA in patients.

The obvious approach of a visual evaluation of fluorescence images requires an intensive training of the evaluator. We hypothesized that a joint affected by RA should show a different dynamic of fluorescence intensity than that of an unaffected joint. Finger tips (FTs), which were assumed to be not affected by RA, were used for normalization. The differences between finger tips and joints are expressed and analyzed in terms of correlation function parameters. This article presents an analysis based on a correlated time series extracted from the recorded set of image frames, which results in a characteristic value for each joint defining its status.

In order to explain the data acquisition procedure, a brief description of the experimental setup is given. More detailed information about the technical specifications can be found in Ref. 9. The computational tools are presented in Sec. 4. The open source package, ImageJ, in conjunction with Java, has been applied to develop algorithms for the evaluation of recorded frame sets and differentiation of healthy and inflamed joints.<sup>14,15</sup>

## 2 Experimental Setup and Data Acquisition

### 2.1 Study Design and Patients

The evaluation reported in Sec. 3 includes data recorded during a prospective trial from a group of 14 healthy volunteers and 16

Address all correspondence to: Thomas Dziekan, Biomedical Optics, Physikalisch-Technische Bundesanstalt, Abbestraße 2-12, Berlin, Berlin 10587 Germany. Tel: +00493034817730; Fax: 00493034817505; E-mail: thomas.dziekan@ptb.de.

**Table 1** Comparison of gender and age between volunteers and patients.

	Participants	Gender		Age		Joints with swelling or pain
		Female	Male	Mean	Min–Max	
Volunteer	12	4	8	24.8	19–50	
patient	16	14	2	62.6	51–74	59.3%

patients with RA. However, only the data of 12 healthy volunteers could be included in further analysis. Two volunteers have been excluded because their fingers were either accidentally contaminated with ICG or their finger nails had a fluorescent nail polish.

The imaging equipment was installed in a clinical environment and measurements on patients and volunteers were performed according to the approval of the ethics committee. An informed consent was obtained from each participant. All patients and volunteers underwent a clinical examination before an optical examination. To perform optical investigations, a dose of 0.1 mg/kg body weight ICG was administered intravenously, at a dose which is lower than that used for other diagnostic applications.<sup>16,17</sup>

As described by Mothes et al.,<sup>17</sup> fluorescence angiography using ICG has been proposed as a helpful indicator of free-flap perfusion in tissue transfers to the outer body. The dye is approved for use in cardiac and liver function diagnostics (Pulsion Medical Systems AG, Munich, Germany).

Table 1 summarizes the data of volunteers and patients with rheumatoid arthritis. It is worth noting that there is a strong difference in age between volunteers and patients. It is not clear to us whether this circumstance may have an impact or not.

### 3 Data Acquisition

Optical excitation of the circulating contrast agent during measurements was achieved with a light-emitting diode (LED) array as an IR-light source, illuminating the field of view (1200 cm<sup>2</sup>, 400  $\mu$ W/cm<sup>2</sup>). An electron multiplying charge coupled device (EMCCD) camera was used to record the emitted fluorescence light with a surface spatial resolution of 2 pixels/mm. The exposure time of the camera was 130 ms. Kinetics of inflow and distribution of ICG were followed over a 10 min period after bolus injection by recording images with a rate of 4 frames/s. The hands of the investigated persons have been confined in a mask in order to suppress motion artifacts. The recorded frames have been corrected for light source fluctuation and illumination inhomogeneities.<sup>9</sup>

The data analysis presented in Sec. 4 is based on a time series of fluorescence intensities measured for each joint and finger tip of the hands. To this end, a circular region of interest (ROI) was defined around each joint, in which the 90th percentile of the count rate of the fluorescence intensity was determined (Fig. 1). The area of the circular ROIs was chosen after inspection of recorded data sets in order to safely cover the area of a certain type of joint with one size in all volunteers and patients. The investigations have been carried out with ROIs of 20 pixels in diameter placed over all finger tips. The diameter of ROIs over

distal interphalangeal (DIP) joints was 24 pixels, over proximal interphalangeal (PIP) joints 28 pixels, and over metacarpophalangeal interphalangeal (MCP) joints 30 pixels. The diameter of ROIs in the small fingers was 20 pixel for DIP joints, 24 pixel in PIP joints, and 30 pixel in MCP joints. The time course of the fluorescence intensity in the ROI covering a joint was obtained by evaluation of the stack of subsequently taken frames. ROIs have been placed over all DIP joints, PIP joints, MCP joints, and finger tips.

By choosing the 90th percentile for evaluating the influence of high or low intensity outliers of all kinds was diminished. Throughout the stack of frames, the size of an ROI was fixed and ideally the position of the ROI follows possible motion of the enclosed joint. Due to the preformed support for the hand, only a few test subjects showed motion artifacts which could be corrected interactively. An automatic readjustment to ensure congruent placement of the ROIs over the joints, such as registering the stack of frames or joint tracking, was not necessary. Figure 2 shows a representative course of the fluorescence intensity in the finger tip and the PIP joint of a right index finger of a patient. The shape of the curve is similar for all joints in patients and volunteers. The measured fluorescence intensity in an ROI is composed of fluorescence originating from excited dye, not only in tissue, but also in arteries loading the area with dye and veins draining the area from dye. Due to the design of the human blood circuit, the effect of superposition is stronger in the proximal located MCP joint than the distal located PIP and DIP joints. Therefore, in comparison to the shown PIP-joint curve, the DIP joint curves are, in general, narrower and the curves in MCP joints show an increased half width. Within the investigated group of volunteers and patients, the recorded maxima

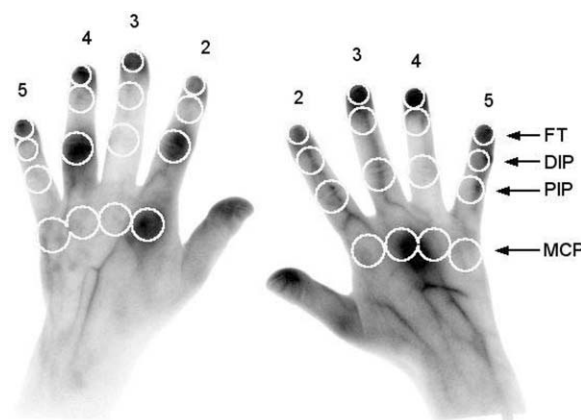


**Fig. 1** Placement of ROIs over FTs, DIP, PIP, and MCP joints.

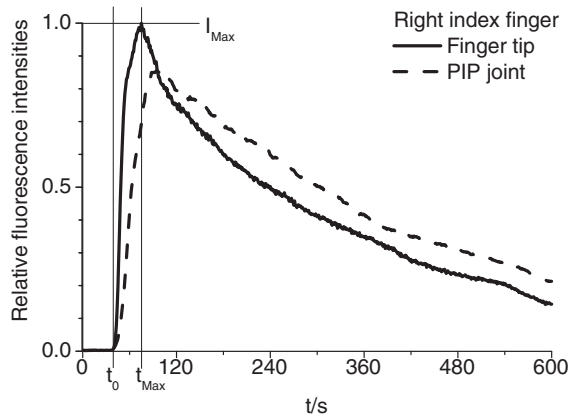


**Fig. 2** Time course of the fluorescence intensity in ROIs of a finger tip and a PIP joint of the right index finger of a RA patient divided by the maximum intensity in the finger tip.

of fluorescence intensity are not significantly higher in patients compared to volunteers.

## 4 Data analysis

### 4.1 Normalization

The dye ICG is mostly bound to blood plasma proteins,<sup>10</sup> and therefore, confined to the vascular system. The fluorescence of ICG recorded with our imaging system is therefore a measure of the vascularization in skin and tissue. However, the fluorescence intensity emitted from the surface of the hand is a two-dimensional (2D) projection of fluorescence photons from different depths in the hand. The dynamics of the ICG concentration at the point of observation is strongly dependent on the physiology of the blood circulation of the investigated person. Therefore, the measure is relative and not directly comparable between individuals. Already in the group of volunteers, fluorescence intensities of joints recorded as described in Sec. 3, show large variations in the time courses such as onset or maxima of fluorescence intensity. The onset time  $t_0$  (see Fig. 2) of the strong increase in fluorescence intensity after the bolus injection in the PIP-ROIs varied, e.g., between 30 and 55 s. All recorded data sets showed a detectable increase in fluorescence intensity, always later than 20 s after bolus injection. Therefore, the onset time  $t_0$  was defined as the time when the sliding average over 3 s (12 data points) of the intensity is increased by more than 30% over the average signal of the first 20 s. At bolus arrival, the intensity increases within 1 or 2 s by 1 order of magnitude. The time  $t_{max}$  between bolus injection and occurrence of the maximum of fluorescence intensity in the PIP joints ranges between 80 and 240 s. The corrected maxima of fluorescence intensity are between 1600 and 5700 counts.

These strong individual blood flow properties have to be corrected to allow the comparison of joints from volunteers and patients with RA. Therefore, a normalization of the fluorescence intensities measured in the ROIs is necessary. For this purpose, we used the finger tips, an area unaffected by rheumatoid arthritis, as a measure of the input function of fluorescence intensity close to the finger joints. Due to the small spatial separation between the finger tip and corresponding joints, only the local differences in the dye concentration are of importance. Other

effects such as the exponential decay of the fluorescence intensity caused by the ICG liver clearance are negligible.

To further reduce the influence of the individual blood circulation, in particular to get rid of the individual time between bolus injection and its appearance in the ROIs, the time  $t_0$  was always used as a reference starting point for further evaluation of each time series, i.e., all data points with times  $t < t_0$  have been removed, and the time scale was shifted to  $t' = t - t_0$ . Furthermore, the length of the analyzed time series has been restricted to 480 s.

### 4.2 Time Dependent Properties and Correlation

We defined a joint status based on fluorescence intensity ratios between the values of a joint and its corresponding finger tip. In a first approach, based on the experiences from our previous work,<sup>8</sup> different relative fluorescence parameters of such types (i.e., intensities of ROIs normalized to that of the finger tip) have been calculated from the raw data of the time series. For instance, the maxima, the means, and the increasing and decreasing slopes, have been computed and evaluated.

In the present study, these approaches did not very well discriminate volunteers and patients, when compared with the individual clinical diagnosis. Figure 3 shows, as an example, the cumulative frequency of the normalized means of fluorescence intensities of PIP-joints of volunteers and patients. The curves for volunteers and patients strongly overlap. Subsequently, sensitivity and specificity as a function of the normalized mean have been derived from the cumulative frequency plots shown in Fig. 3, and plotted as receiver operating characteristics (ROC) curves. A ROC curve visualizes the characteristic interplay of sensitivity and specificity depending on a discriminator as a parameter. The diagram indicates a certain sensitivity for a given false positive rate (1-specificity). The coordinates of each point in the diagram are sensitivity and 1-specificity for the same discriminator. A value close to 0.5 for the area under the ROC-curve (ROC-AUC) means a complete overlap of the two groups to be

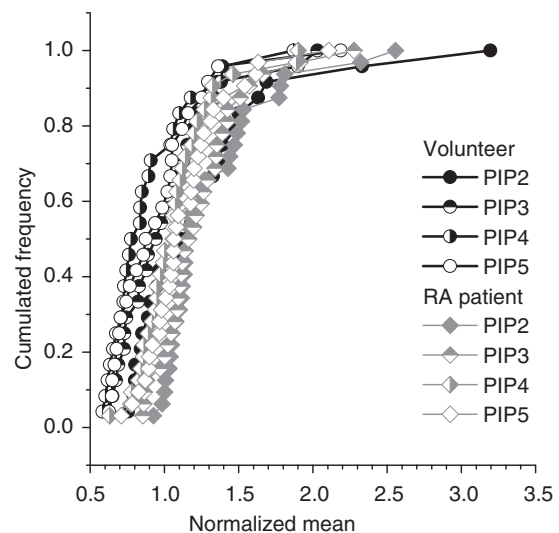


**Fig. 3** Normalized cumulative frequencies versus normalized means of fluorescence intensities from PIP joints of healthy volunteers and RA patients.

distinguished. The closer the value of the AUC comes to 1, the better the two groups are separated. An AUC-value close to 1 means the graph has a sensitivity of 100% almost everywhere.

The AUC of the ROC curve, based on sensitivity and specificity derived from the data of Fig. 3, resulted in AUC-values below 0.7. We concluded from these results that the ratio analysis taking into account simple time-integrated values, or values at certain times, is of poor discriminative power, since the available time evolution has been not considered. The more the dynamics of intensities in the finger tip and joints differ, the more likely it is that the joint is affected.

As an improvement, we suggest, therefore, to include an analysis of the time information by correlating the time courses of the fluorescence intensities of a joint and its corresponding finger tip.

The correlation function  $\rho_{FT,Joint}(\Delta t)$  for a time shift  $\Delta t$  between the time-series of fluorescence intensities in the finger tip  $I_{FT}(t_n)$  and a joint  $I_{Joint}(t_n)$  is defined as:

$$\rho_{FT,Joint}(\Delta t) = \frac{\langle I_{FT}(t_n)I_{Joint}(t_n + \Delta t) \rangle}{\sqrt{\langle I_{FT}(t_n)^2 \rangle \langle I_{Joint}(t_n + \Delta t)^2 \rangle}}. \quad (1)$$

The brackets  $\langle \cdot \cdot \cdot \rangle$  represent the time averaging of the enclosed entities. The correlation function has been calculated for positive and negative time shifts up to the maximum length of the prepared time series (480 s).

As for the treatment of raw data ratios mean, maxima, and variance of the correlation function have been analyzed and yielded the best results for the variance. The bolus distribution and liver uptake effects have been eliminated as before by dividing the variances for the joints with one of the corresponding finger tips:

$$\hat{\rho} = \frac{\langle (\rho_{FT,Joint}(\Delta t) - \langle \rho_{FT,Joint}(\Delta t) \rangle)^2 \rangle}{\langle (\rho_{FT,FT}(\Delta t) - \langle \rho_{FT,FT}(\Delta t) \rangle)^2 \rangle}. \quad (2)$$

To demonstrate the proposed method, time courses of the fluorescence signal observed in PIP joints have been analyzed. This group of joints contained a fairly high number of inflamed joints within the investigated group of patients. The number of investigated PIP joints is given in Table 2.

In Fig. 4, the cumulative frequency of normalized variances of the correlation function for all PIP joint groups of volunteers and patients are plotted. It can be seen that the normalized values for volunteers show lower values than those for patients.

It is obvious from Fig. 4, however, that the groups of volunteers and patients still overlap. However, the notched box

**Table 2** Number of investigated joints in patients (32) including the clinical findings for swelling and/or pain at the time point of NIR imaging.

Finger	Without pathological findings	Swelling and/or pain
Index	14	18
Middle	10	22
Ring	14	18
Small	17	15

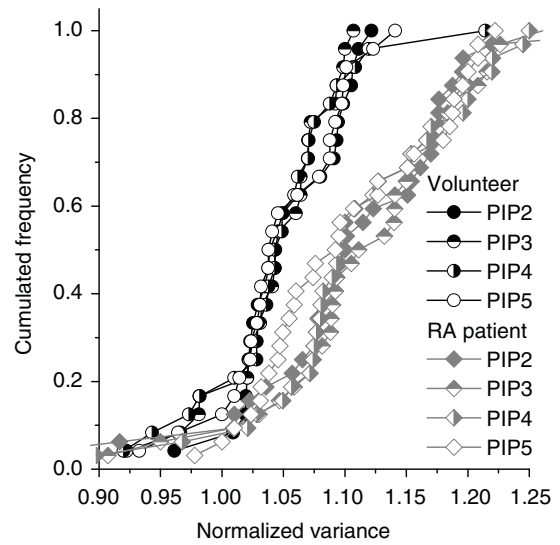


**Fig. 4** Normalized cumulative frequency versus normalized variances of the correlation function from PIP joints of healthy volunteers and RA patients.

plots presented in Fig. 5 show that the medians for volunteers and patients are clearly separated. These findings support that—within the evaluated group of individuals—our method based on variances of normalized correlation functions, allows to discriminate joints of RA patients from the joints of volunteers. For RA patients, a good separation between asymptomatic and inflamed joints was not possible. It must be noted that the latter result is mainly a consequence of the “gold standard” we had to compare with, but probably not a deficiency of our method. The comparison with inclusion criteria for RA (our quasigold standard) gave a result for all joints per patient only, i.e., all joints of RA patients were treated as having potentially inflamed joints without further differentiation. The worst separation with a poor AUC = 0.71 was, e.g., obtained for the group of PIP joints from the small fingers because a fairly high number of these joints

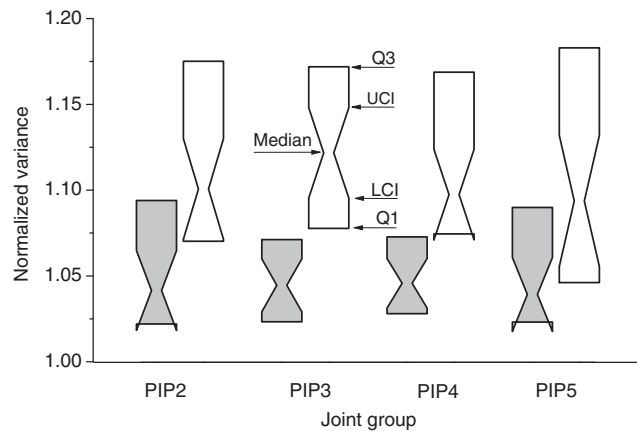


**Fig. 5** Notched box plots of normalized variances of the correlation function from PIP joints of healthy volunteers (filled boxes) and RA patients (open boxes). Two medians are significantly different if their lower and upper confidence intervals (LCI, UCI) do not overlap, as e.g., with PIP2, PIP3, and PIP4.

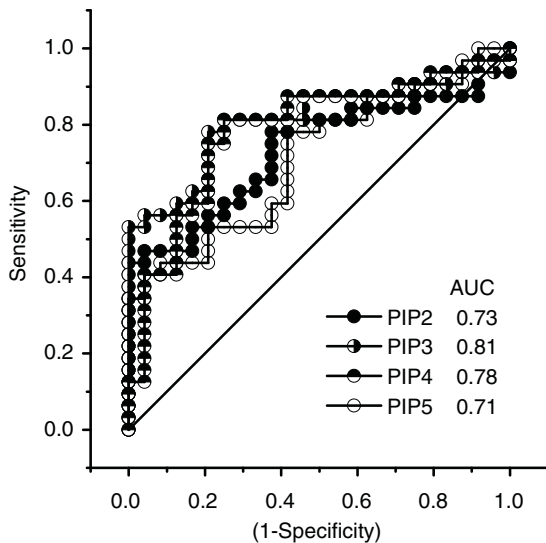


**Fig. 6** ROC curves computed from normalized variances of the correlation function shown in Fig. 4. The inset table contains particular values derived from the ROC curves.

(17 out of 32) was without acute swelling or pain, but classified as RA because of the overall assessment.

The wide spreading of the presented results is caused by the individual physiological variation in vascular or skin properties, which are not completely eliminated by the proposed normalization procedure. The normalization areas are placed on finger nails, which we assume not to be strongly age dependent or having strongly varying tissue properties below the nail. The difference in age and different thicknesses of subcutaneous adipose tissue<sup>18</sup> between volunteers and patients, which causes different optical properties, are not yet taken into account.

ROC curves have been plotted and the area under the AUC was calculated in order to quantify the discriminating power. The results are presented in Fig. 6. The best discrimination has been found for the PIP joints of the middle finger with an AUC of 0.81. Generally, normalized cumulative frequencies of normalized variances show an improved discrimination power compared to raw data analysis (see Figs. 3 and 4).

## 5 Summary

The normalized variances of the correlated time series extracted from contrast enhanced fluorescence imaging data are applicable to discriminate joints of healthy volunteers well from joints of patients with rheumatoid arthritis. Analyzing the fluorescence image series of the PIP joints has been clearly demonstrated. The MCP joints show similar results. DIP joints have not been analyzed because the number of joints affected by rheumatoid arthritis was too small.

The normalized variances of the correlation functions of fluorescence intensities of finger tips and associated joints are determined by a robust, parameter-free algorithm. Only the check of the correct placement of the ROIs requires an operator. More sophisticated evaluation procedures or imaging methods may improve the diagnostic power. Simulation of optical properties of finger joints and the pharmacokinetic behavior of the dye bolus are under way, which might provide further improvements.

## Acknowledgments

We thank D. Streitbürger from the IT help desk of the Physikalisch-Technische Bundesanstalt for his valuable support during the ImageJ-Plugin implementation. This work was supported by the European Regional Development Fund (EFRE) and by the Investitions Bank Berlin (IBB).

## References

1. J. Bernhard and P. M. Villiger, "Rheumatoide arthritis: pathogenese und pathologie." *Schweiz Med. Forum.* **2001**(8), 179–183 (2001) (in German).
2. S. Merkesdal, J. Ruof, O. Schoffski, K. Bernitt, H. Zeidler, and W. Mau, "Indirect medical costs in early rheumatoid arthritis: composition of and changes in indirect costs within the first three years of disease," *Arthritis Rheum.* **44**(3), 528–534 (2001).
3. P. Emery, "Early rheumatoid arthritis: therapeutic strategies," *Scand. J. Rheumatol. Suppl.* **100**, 3–7 (1994).
4. M. Backhaus, T. Kamradt, D. Sandrock, D. Loreck, J. Fritz, K. J. Wolf, J. H. Raber, B. Hamm, G.-R. Burmester, and M. Bollow, "Arthritis of the finger joints: a comprehensive approach comparing conventional radiography, scintigraphy, ultrasound, and contrast-enhanced magnetic resonance imaging," *Arthritis Rheum.* **42**(6), 1232–1245 (1999).
5. C. Bremer, V. Ntziachristos, and R. Weissleder, "Optical-based molecular imaging: contrast agents and potential medical applications," *Eur. Radiol.* **13**(2), 231–243 (2003).
6. A. Wunder, R. H. Straub, S. Gay, J. Funk, and U. Muller-Ladner, "Molecular imaging: novel tools in visualizing rheumatoid arthritis," *Rheumatology (Oxford)*, **44**(11), 1341–1349 (2005).
7. T. Fischer, I. Gemeinhardt, S. Wagner, D. von Stieglitz, J. Schnorr, K. G. A. Herrmann, B. Ebert, D. Petzelt, R. Macdonald, K. Licha, M. Schirner, V. Krenn, T. Kamradt, and M. Taupitz, "Assessment of unspecific near-infrared dyes in laser-induced fluorescence imaging of experimental arthritis," *Acad. Radiol.* **13**(1), 4–13 (2006).
8. T. Fischer, B. Ebert, J. Voigt, R. Macdonald, U. Schneider, A. Thomas, B. Hamm, and K. G. A. Herrmann, "Detection of rheumatoid arthritis using nonspecific contrast enhanced fluorescence imaging," *Acad. Radiol.* **17**(3), 375–381 (2010).
9. B. Ebert, T. Dziekan, C. Weissbach, M. Mahler, M. Schirner, B. Berlin, D. Bauer, J. Voigt, M. Berliner, M. L. Bahner, and R. Macdonald, "Detection of rheumatoid arthritis in humans by fluorescence imaging," *Proc. SPIE* **7555**, 75550H (2010).
10. K. Kamisaka, Y. Yatsuji, H. Yamada, and H. Kameda, "The binding of indocyanine green and other organic anions to serum proteins in liver diseases," *Clinica. Chimica. Acta.* **53**, 255–264 (1974).
11. S. Yoneya, T. Saito, Y. Komatsu, I. Koyama, K. Takahashi, and J. Duvoll-Young, "Binding properties of indocyanine green in human blood," *Invest. Ophthalm. Visual Sci.* **39**, 1286–1290 (1998).
12. T. Desmettre, J. M. Devoisselle, and S. Mordon, "Fluorescence properties and metabolic features of indocyanine green (ICG) as related to angiography," *Surv. Ophthalmol.* **45**(1), 15–27 (2000).
13. Y. Kang, M. Choi, J. Lee, G. Y. Koh, K. Kwon, and C. Choi, "Quantitative analysis of peripheral tissue perfusion using spatiotemporal molecular dynamics," *PLoS One* **4**, e4275 (2009).
14. W. S. Rasband, *ImageJ*, U. S. National Institutes of Health, Bethesda, Maryland, 1997–2009, <http://rsb.info.nih.gov/ij/>.
15. M. D. Abramoff, P. J. Magelhaes, and S. J. Ram, "Image processing with ImageJ," *Biophotonics Int.* **11**(7), 36–42 (2004).
16. H. Mothes, T. Dinkelaker, T. Dönicke, R. Friedel, G. O. Hofmann, and O. Bach, "Outcome prediction in microsurgery by quantitative evaluation of perfusion using ICG fluorescence angiography," *J. Hand Surg. Eur.* **34**(2), 238–246 (2009).
17. H. Mothes, T. Dönicke, R. Friedel, M. Simon, E. Markgraf, and O. Bach, "Indocyanine-green fluorescence video angiography used clinically to evaluate tissue perfusion in microsurgery," *J. Trauma* **57**(5), 1018–1024 (2004).
18. S. M. C. Lee and M. S. F. Clarke, "Elevated skin blood flow influences near infrared spectroscopy measurements during supine rest," NASA/TP-2004-213149, S-942 (2004).